Supplementary Information

Chemically Defined and Small Molecule-Based Generation of Human Cardiomyocytes

Paul W. Burridge[1-3], Elena Matsa[1-3], Praveen Shukla[1-3], Ziliang C. Lin[4], Jared M. Churko[1-3], Antje D. Ebert[1-3], Feng Lan[1-3], Sebastian Diecke[1-3], Bruno Huber[1-3], Nicholas M. Mordwinkin[1-3], Jordan R. Plews[1-3], Oscar J. Abilez[1-3], Bianxiao Cui[5], Joseph D. Gold[1], & Joseph C. Wu[1-3]

[1]Stanford Cardiovascular Institute, [2]Institute for Stem Cell Biology and Regenerative Medicine, [3]Department of Medicine, Division of Cardiology, [4]Department of Applied Physics, [5]Department of Chemistry, Stanford University School of Medicine, Stanford, California, USA

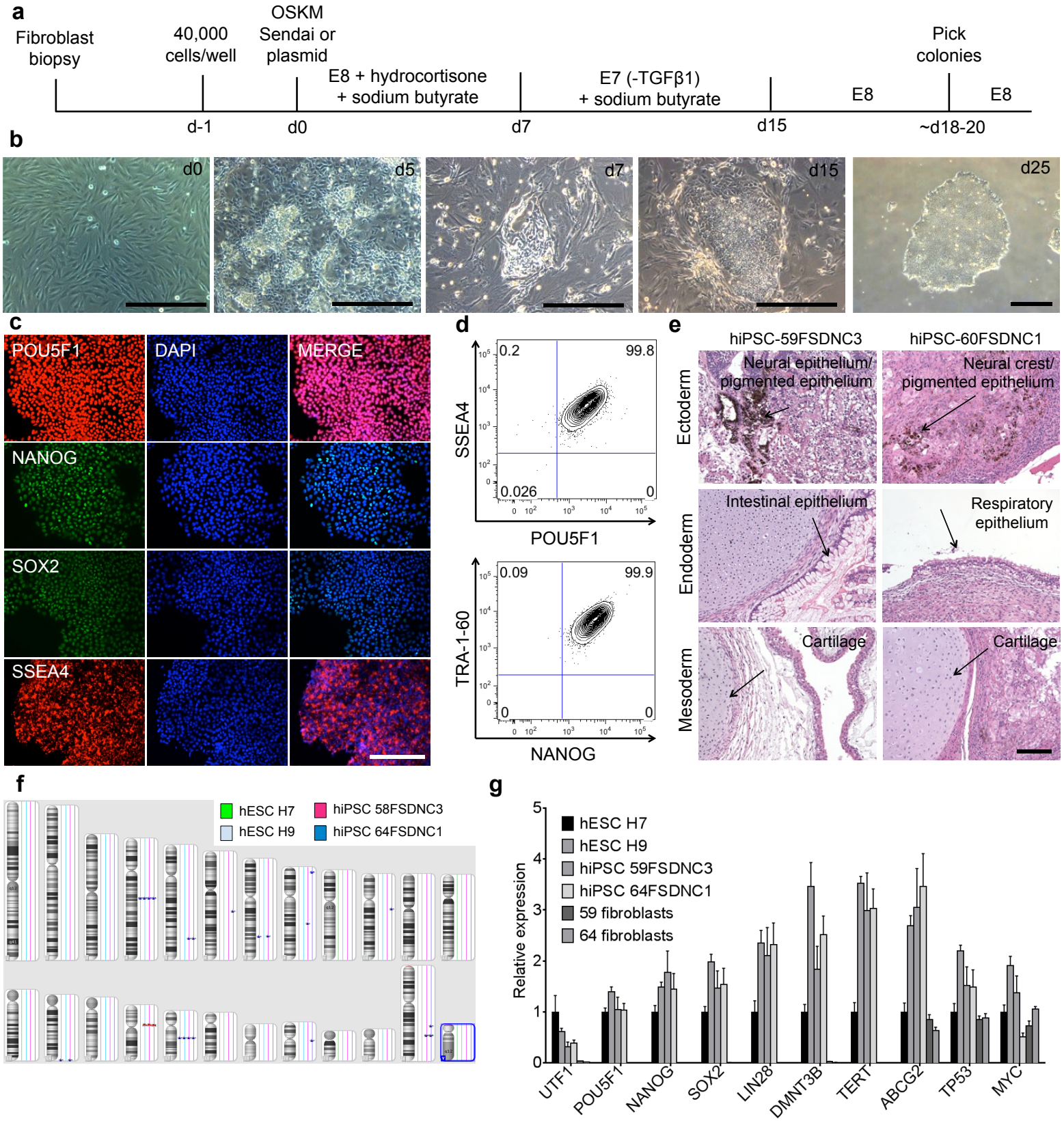

Supplementary Figure 1 | Generation of hiPSCs using a chemically defined, synthetic matrix, integration-free methodology. **a)** Timeline of strategy for chemically defined fibroblast reprogramming and phase contrast images of cells during reprogramming. Eleven cell lines were made using this strategy from fibroblasts or peripheral blood mononuclear cells, reprogrammed with either Sendai virus (*POU5F1 [OCT4], SOX2, KLF4, MYC*), episomal plasmids (*OCT4, SOX2, KLF4, MYCL, LIN28*, short hairpin p53), or a single ~9kb codon optimized mini-intronic plasmid (*OCT4, SOX2, KLF4, MYC*). Scale bar, 50 μm. **b)** Phase contrast images of fibroblasts during reprogramming (cell line 59FSDNC3 shown as an example). **c)** Immunofluorescence staining for pluripotency marker expression. Scale bar, 12.5 μm. **d)** Flow cytometry assessment of pluripotency markers. **e)** Teratoma assay demonstrating cell types from all three germ layer lineages. Scale bar, 50 μm. **f)** SNP karyotype of hESC (H7 and H9) and hiPSC (59FSDNC3 and 60FSDNC1) lines demonstrating normal karyotype of hiPSC after reprogramming. **g)** Real time RT-PCR assessment of genes associated with pluripotency in hiPSC lines (59FSDNC3 and 64FSDNC1), and fibroblasts they were derived from, relative to H7 hESC. Error bars represent S.D. from experimental quadruplicates.

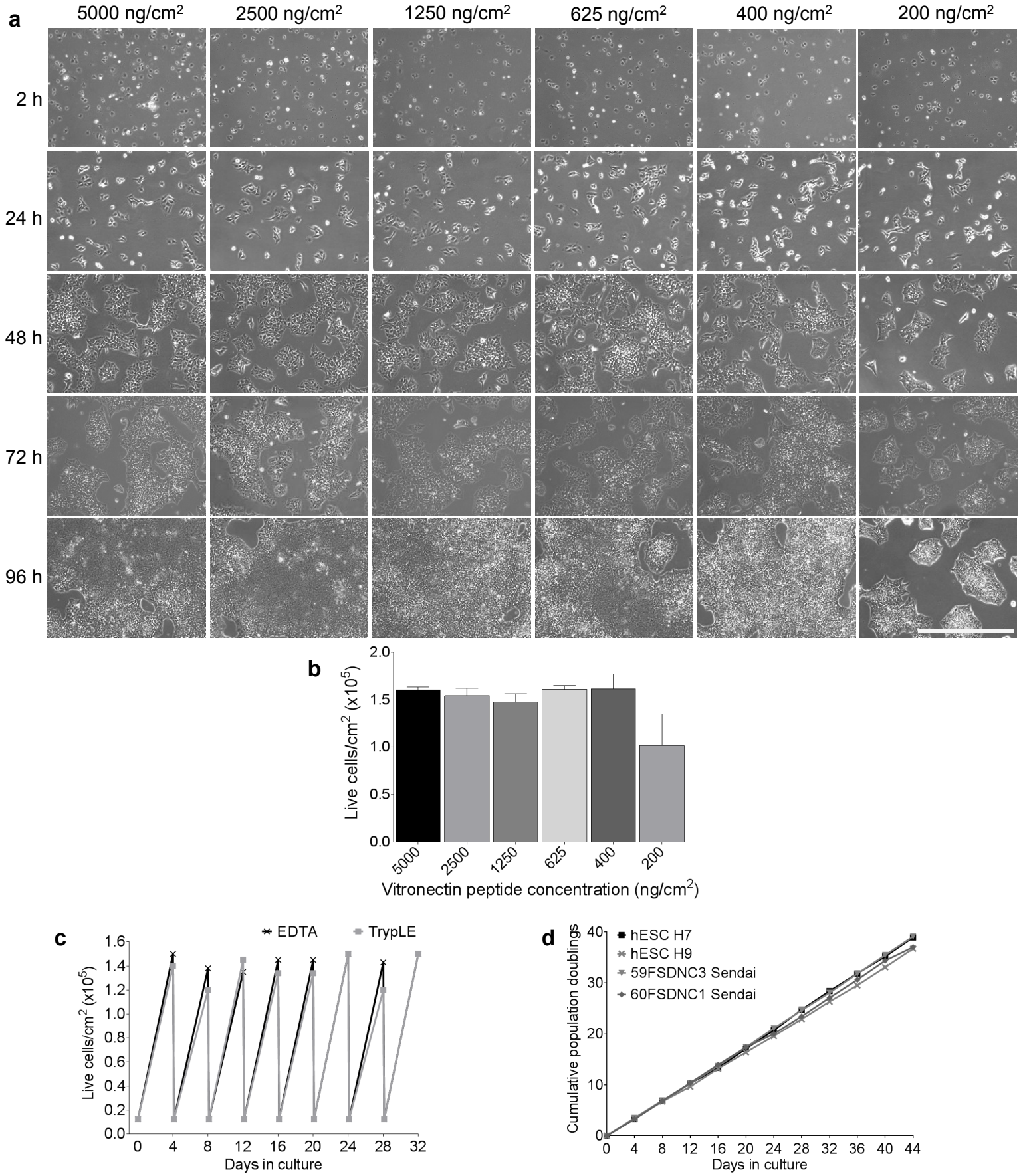

Supplementary Figure 2 | Growth of hiPSCs in chemically defined medium on a synthetic vitronectin peptide matrix. **a)** Phase contrast images of hiPSC line 59FSDNC3 grown on increasingly lower concentrations of vitronectin peptide. A concentration of 625 ng/cm^2 was used for subsequent studies. Scale bar, 100 µm. **b)** Cell yields after seeding on vitronectin peptide at 1.25 × 10^4 cells/cm and 96 h of growth, *n* = 3. Error bars represent S.E.M. Cost of vitronectin peptide at a concentration of 625 ng/cm^2 were equivalent to standard costs of Matrigel. **c)** Comparison of EDTA and TrypLE for passage on reproducibility of growth rate, cells were split 1:12 for EDTA or counted and plated at 1.25 × 10^4 cells/cm^2 for TrypLE. **d)** Cumulative population doublings of two hESC lines (H7 and H9) and two hiPSC lines (59FSDNC3 and 64FSDNC1) grown in E8 medium on vitronectin peptide.

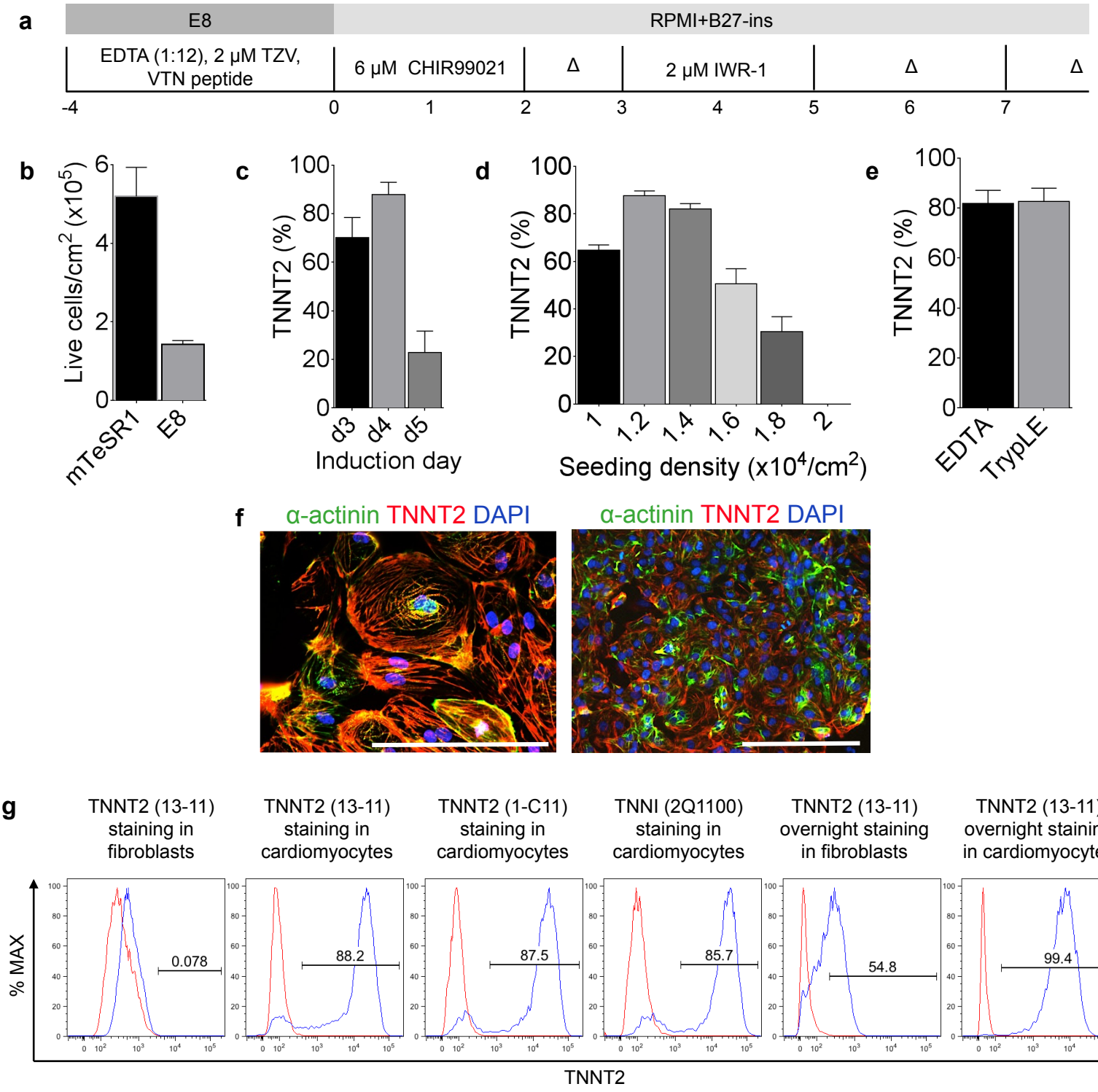

Supplementary Figure 3 | Modification of existing RPMI+B27-ins small molecule-based differentiation methodology for pluripotent cells cultured under chemically defined conditions. **a)** Schematic of modified differentiation protocol. **b)** Yield of live cells after 96 h culture in either mTeSR1 or E8. mTeSR1 cells were seeded at 1.25 x 10^5 cells per cm^2 and E8 cells at 1.25 x 10^4 cells per cm^2, *n* = 3. **c)** Optimization of number of day after passage for highest efficiency cardiac differentiation measured by percentage TNNT2 positive cells assessed by flow cytometry, *n* = 3. **d)** Optimization of seeding density for subsequent differentiation efficacy, *n* = 3. **e)** Effect of clump (EDTA) or single cell (TrypLE) passaging method on subsequent differentiation efficiency. **f)** Immunofluorescence images of cells produced by E8/EDTA/RPMI+B27-ins methodology. Scale bar, 25 μM. **g)** Optimization of cardiac troponin T (TNNT2) flow cytometry staining, to test the specificity of our staining protocol, we stained fibroblasts (45 min primary) with the TNNT2 antibody 13-11 and demonstrated a very minor increase in staining (blue) over the isotype control (red). We also assessed additional monoclonal antibodies for cardiac troponin T (1-C11) and cardiac troponin I (7E147), each from a different manufacturer, and found similar levels of positive cell detection (~85-88%). As part of our optimization, we also assessed overnight primary antibody staining with the TNNT2 13-11 antibody and found that this method gave us significant non-specific staining in fibroblasts and raised the percentage of TNNT2+ cells to >99%. Therefore we adhered to 45 min staining as above.

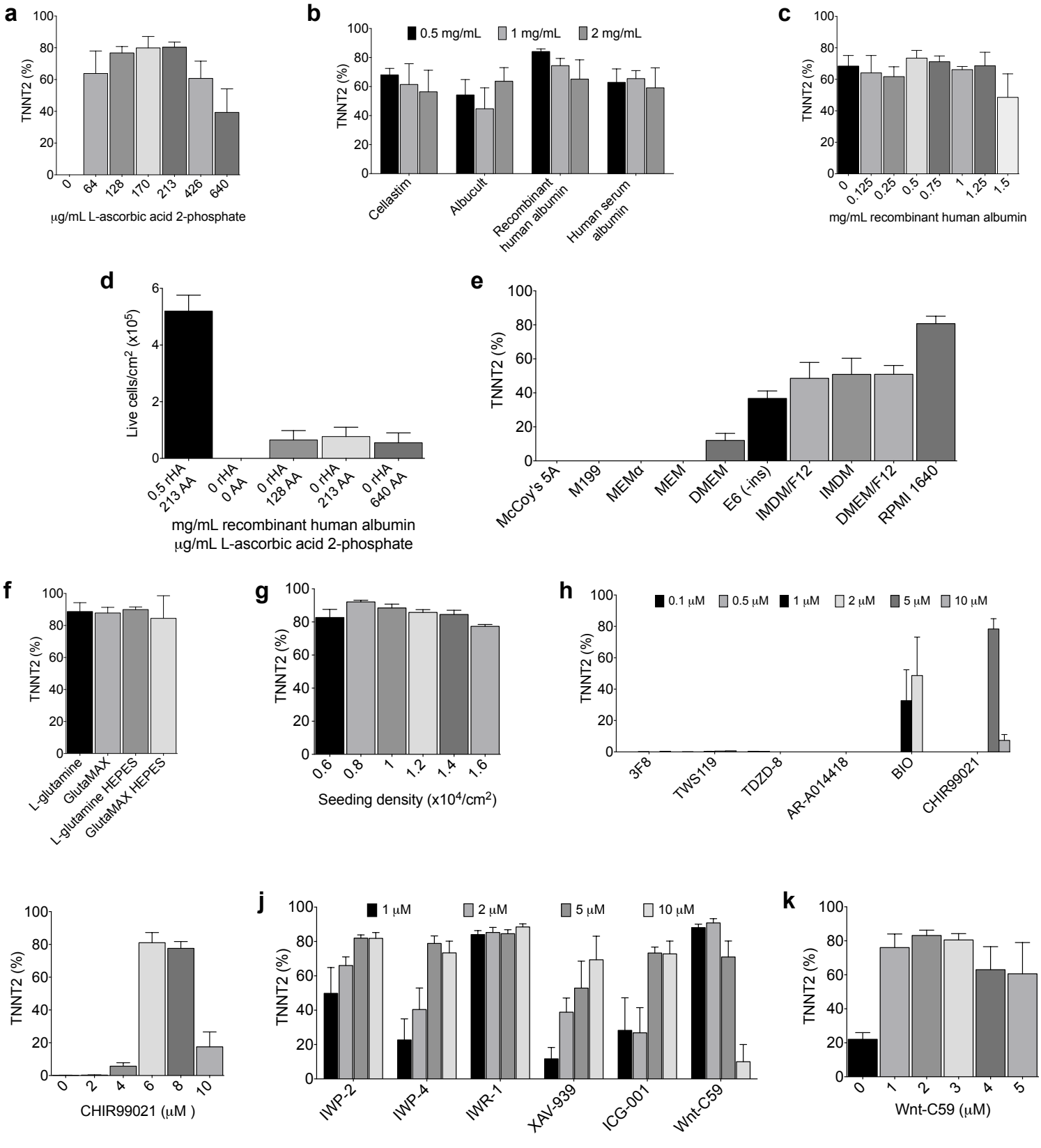

Supplementary Figure 4 | Optimization of chemically defined differentiation media and small molecules. **a)** Optimal dose of L-ascorbic acid 2-phosphate, *n* = 7. **b)** Optimization of recombinant human albumin supplier, *n* = 3. **c)** Optimization of rHA dose, qualitatively 500 μg/mL rHA produced the most suitable contracting monolayers whereas 750 μg/mL and above were more likely to result in the formation of three-dimensional structures, *n* = 7. **d)** Assessment of elimination of recombinant human albumin on cardiomyocyte yield when varying does of L-ascorbic acid 2-phosphate. Replacement of rHA with polyvinyl alcohol (PVA), which prevents shear stress in a similar manner to rHA, combined with varying doses of AA 2-P did not increase differentiation yield. **e)** Optimization of basal media, *n* = 3. **f)** Assessment of different RPMI 1640 media variants, *n* = 3. **g)** Optimization of pluripotent cell seeding density, *n* = 3. **h)** Optimization of GSK3β inhibitor; only BIO and CHIR99021 did not cause total cell death, *n* = 3. **i)** Optimization of CHIR99021 dose, *n* = 4. **j)** Optimization of Wnt inhibitor dose, *n* = 3. **k)** Optimization of Wnt-C59 dose, *n* = 4.

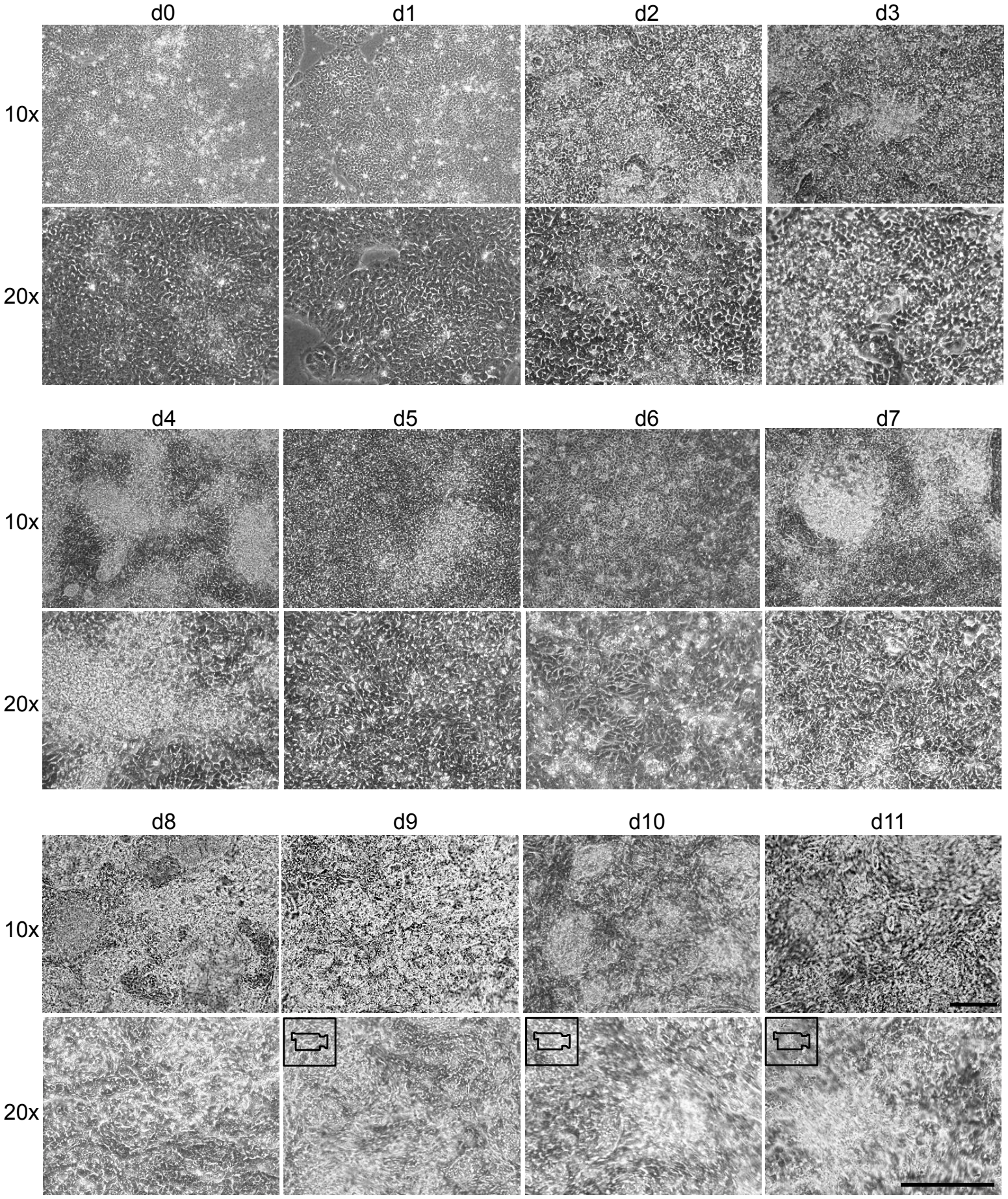

Supplementary Figure 5 | Phase contrast images of hiPSC during chemically defined differentiation. These images demonstrate minimal cell death. Videos of day 9, day 10, and day 11 are provided in Supplementary Videos 1, 2, and 3, respectively. Scale bar, 25 μM.

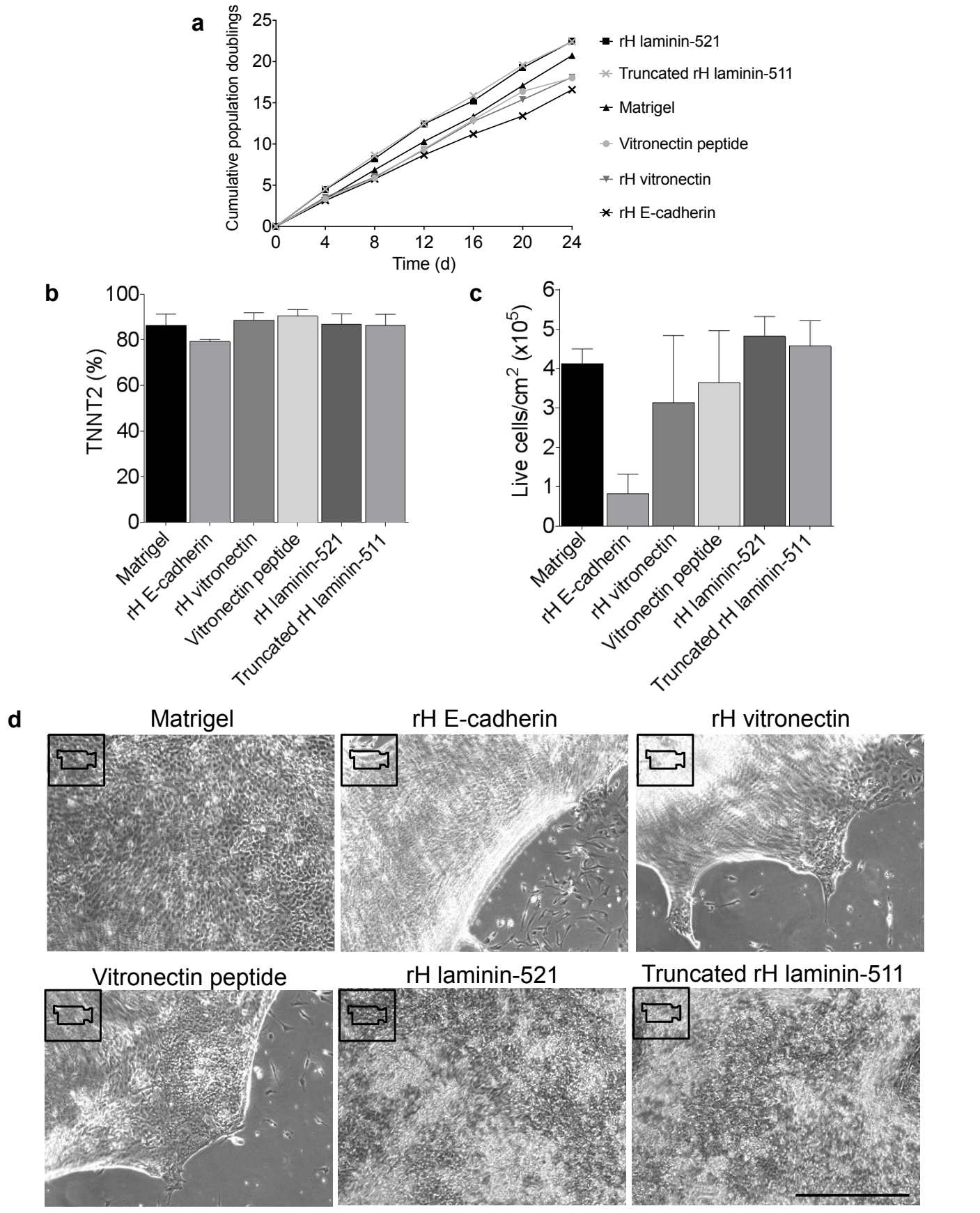

Supplementary Figure 6 | Cardiac differentiation of hiPSC on chemically defined matrices. **a)** Comparison of growth rates of hiPSC line 59FSDNC3 in E8 media on optimal concentrations of various defined matrices: rH laminin-521, 2.5 µg/cm^2; truncated rH laminin-511, 2 µg/cm^2; Matrigel, 9 µg/cm^2; vitronectin pepetide, 625 ng/cm^2; rH vitronectin, 1 µg/cm^2; and rH E-cadherin, 1 µg/cm^2. **b)** Cardiac differentiation efficiency of cells cultured on defined matrices for >6 passages was measured on day 15 by flow cytometry for TNNT2 positive cells, n = 3. **c)** Yield of live cells at day 15 differentiation from cells cultured on various defined matrices, n = 4. **d)** Phase contrast images of day 13 cells demonstrating issues with cell adhesion on some matrices. Of note, combining vitronectin peptides with fibronectin peptides (Pronectin) did not alleviate the adhesion issue. Videos of each are provided in Supplementary Video 4-9. Scale bar, 25 µm.

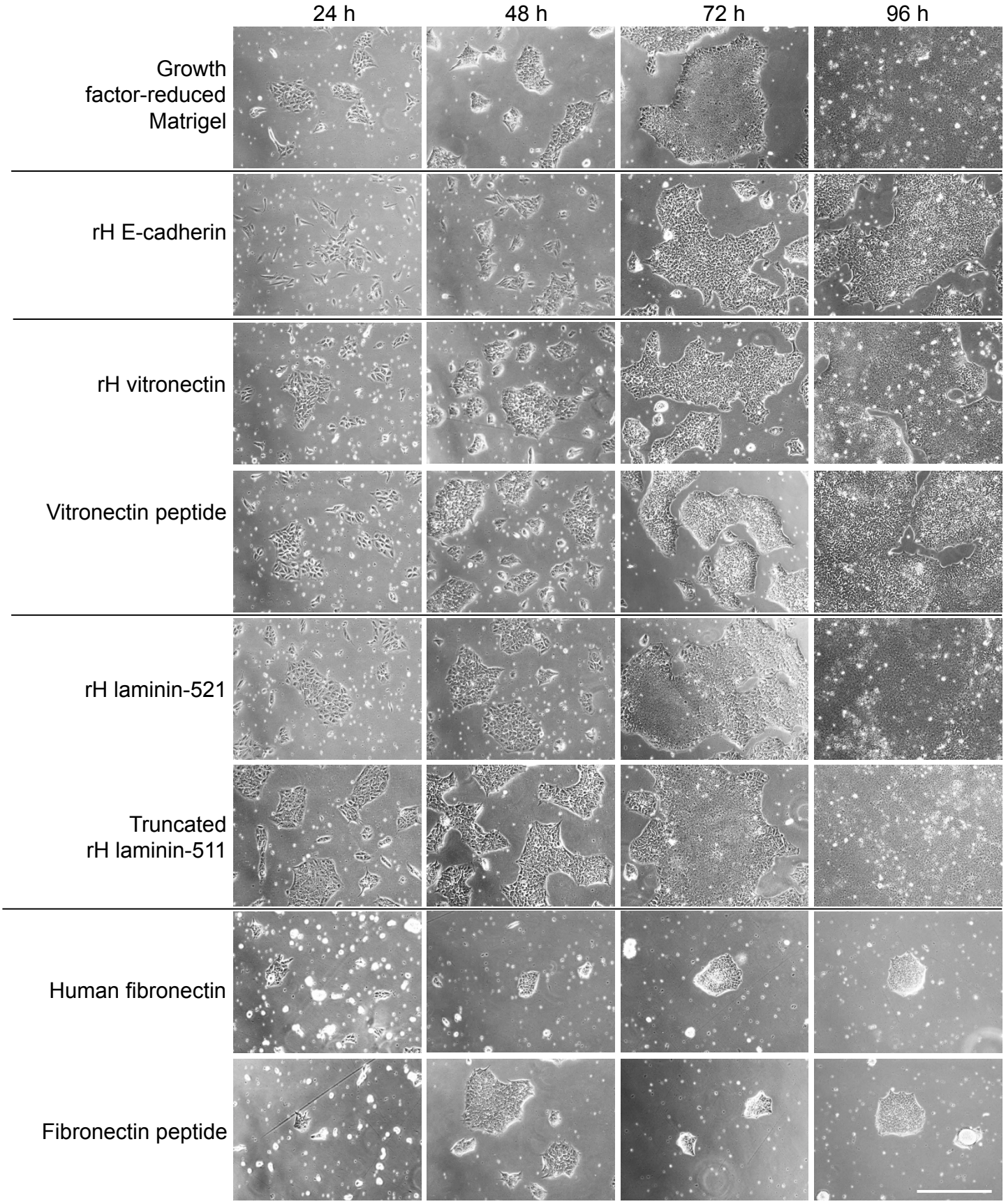

Supplementary Figure 7 | Pluripotent growth of hiPSC in chemically defined medium on chemically defined matrices. Growth rates of 59FSDNC3 hiPSC in modified E8 media on various defined surfaces, compared to Matrigel. Cells were imaged by phase contrast microscopy after 24, 48, 72, and 96 hours of growth with daily media changes. Scale bar, 100 μm.

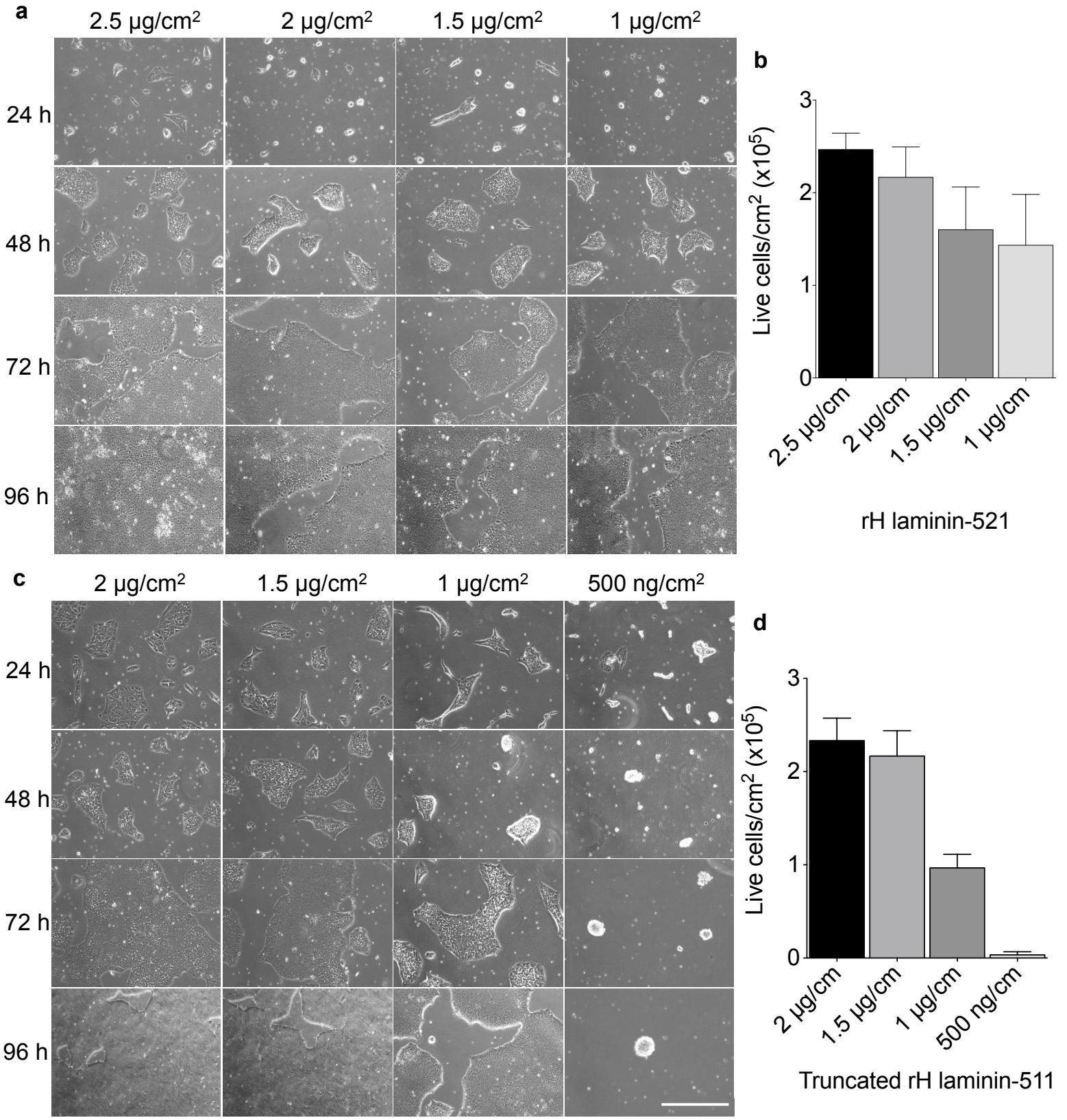

Supplementary Figure 8 | Pluripotent growth of hiPSC on minimal concentrations of laminin matrices. **a)** Comparison of growth rates of 59FSDNC3 hiPSC in E8 medium. Phase contrast images of cells grown on decreasing concentrations of rH laminin-521 for 96 h. Scale bar, 100 µm. **b)** Plot of live cell yields after seeding cells at 1.25 x 10^4 cells per cm^2 and 96 h of growth on laminin-521, *n* = 3 Error bars represent S.E.M. **c)** Phase contrast images of cells grown on decreasing concentrations of truncated rH laminin-511 for 96 h. Scale bar, 50 µm. **d)** Plot of live cell yields after seeding cells at 1.25 x 10^4 cells per cm^2 and 96 h of growth on truncated rH laminin-511, *n* = 3. Error bars represent S.E.M.

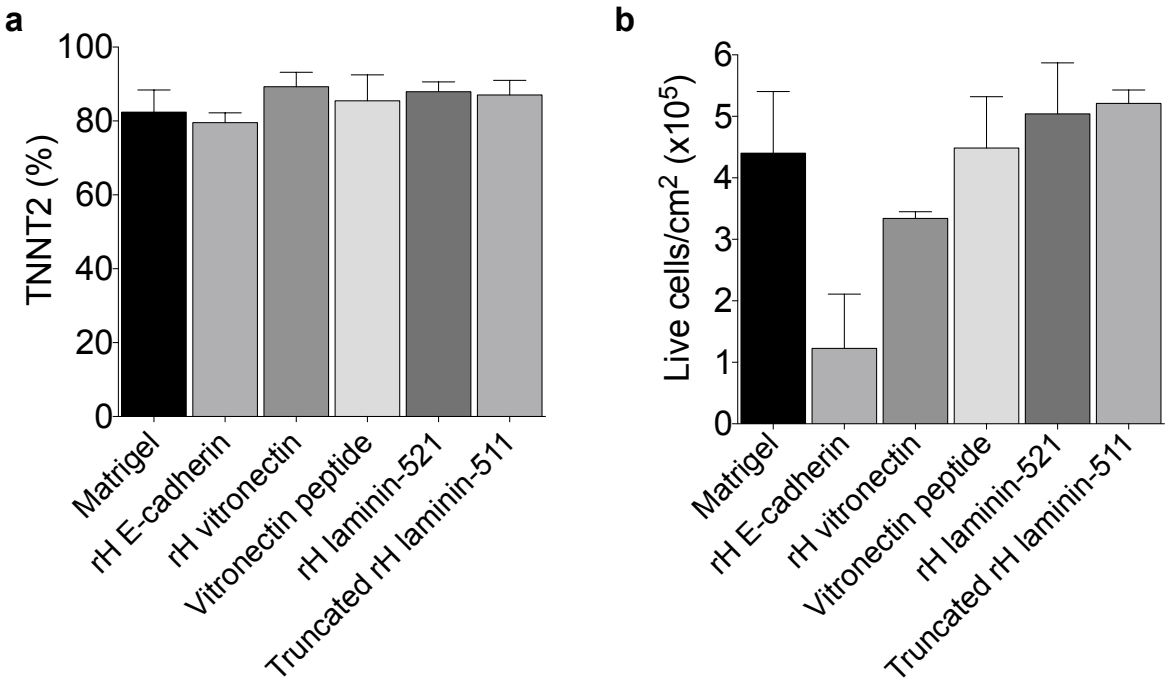

Supplementary Figure 9 | Growth of hiPSC on Matrigel followed by cardiac differentiation on chemically defined matrices. **a)** Cardiac differentiation efficiency of cells cultured on Matrigel then swapped to defined matrices on d−4, measured on day 15 by flow cytometry for TNNT2 positive cells, *n* = 2. **b)** Yield of live hiPSC-derived cardiomyocytes at differentiation day 15 from cells cultured on various defined matrices, *n* = 2.

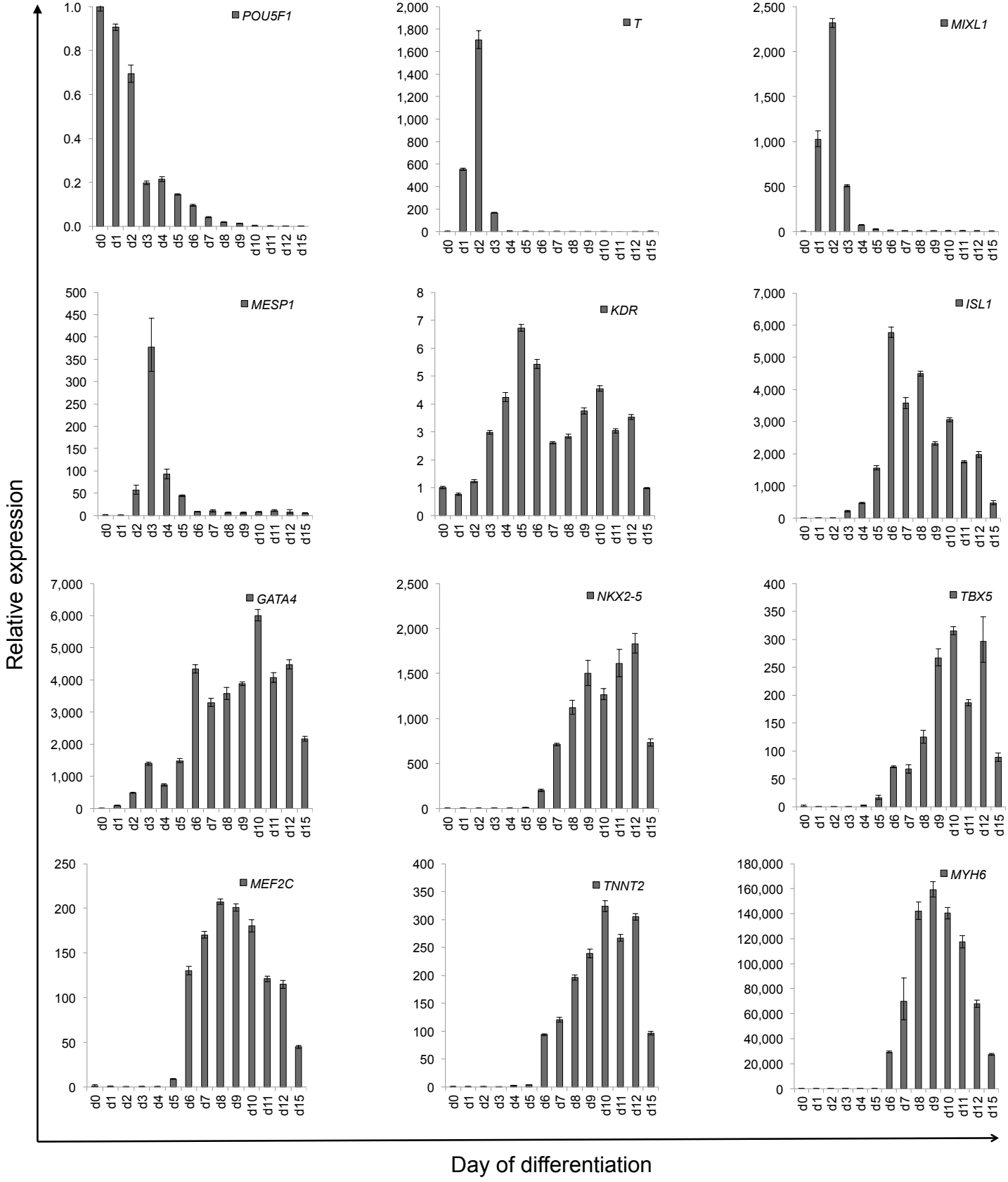

Supplementary Figure 10 | Gene expression during chemically defined cardiac differentiation. Real-time RT-PCR for markers of pluripotency (*POU5F1*), mesoderm (*T and MIXL1*), cardiac mesoderm (*MESP1 and KDR*), committed cardiac progenitors (*ISL1, GATA4, NKX2-5, TBX5, and MEF2C*), and cardiomyocytes (*TNNT2 and MYH6*)**.** Samples used in this analysis were matched pairs for phase contrast images in Supplementary Fig. 5. Error bars represent S.D. of technical quadruplicates.

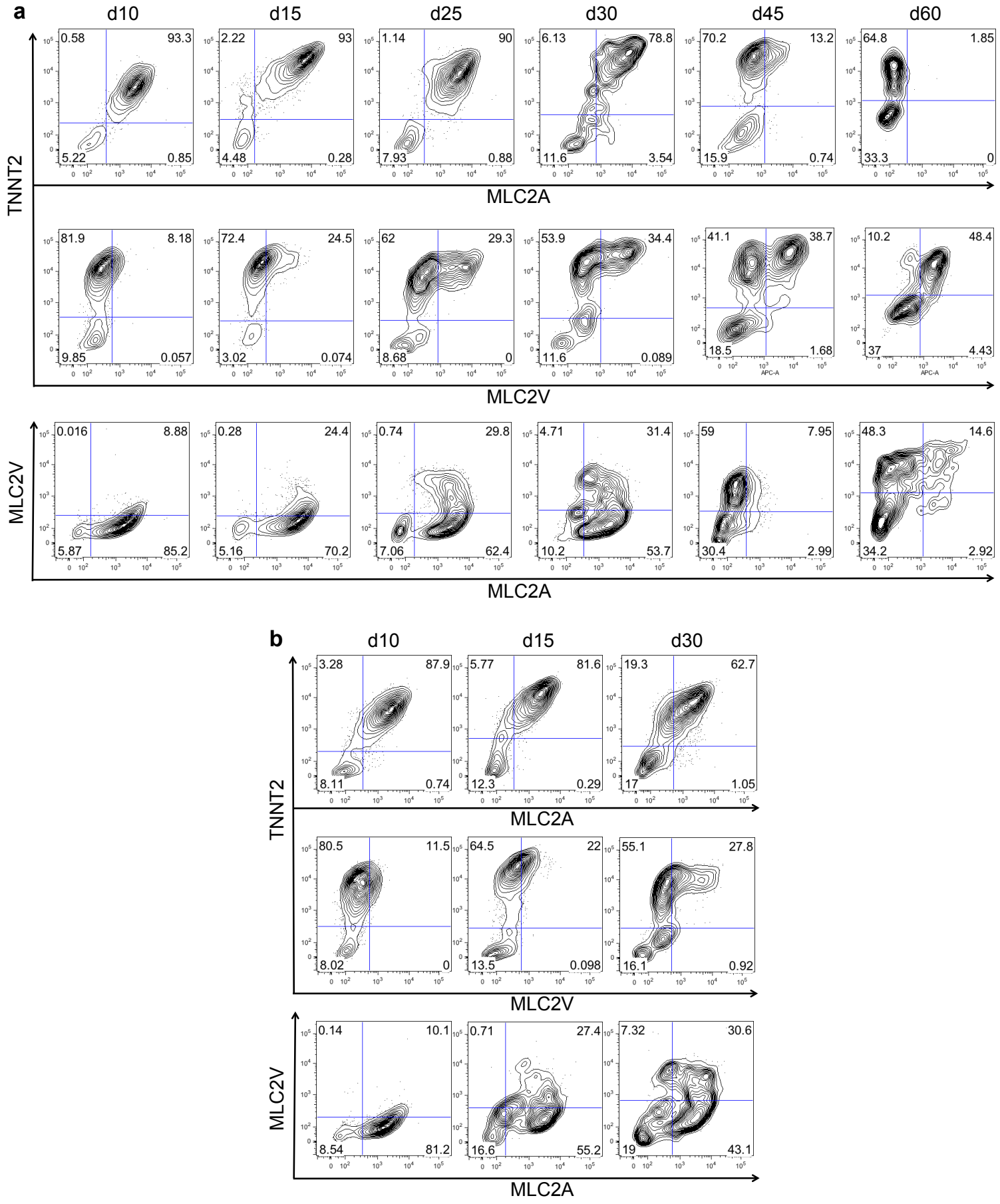

Supplementary Figure 11 | Characterization of atrial vs. ventricular profile of cardiomyocytes produced under chemically defined conditions using flow cytometry. **a)** Flow cytometry assessment of expression of cardiac troponin T (TNNT2), atrial myosin light chain 2 (MLC2A), and ventricular myosin light chain (MLC2V) in cardioymyocytes derived and maintained in CDM3 at differentiation from day 10 through day 60. **b)** Flow cytometry assessment of expression of TNNT2, MLC2V, and MLC2A in cardiomyocytes differentiated using RPMI+B27-ins media at differentiation day 10 through day 30.

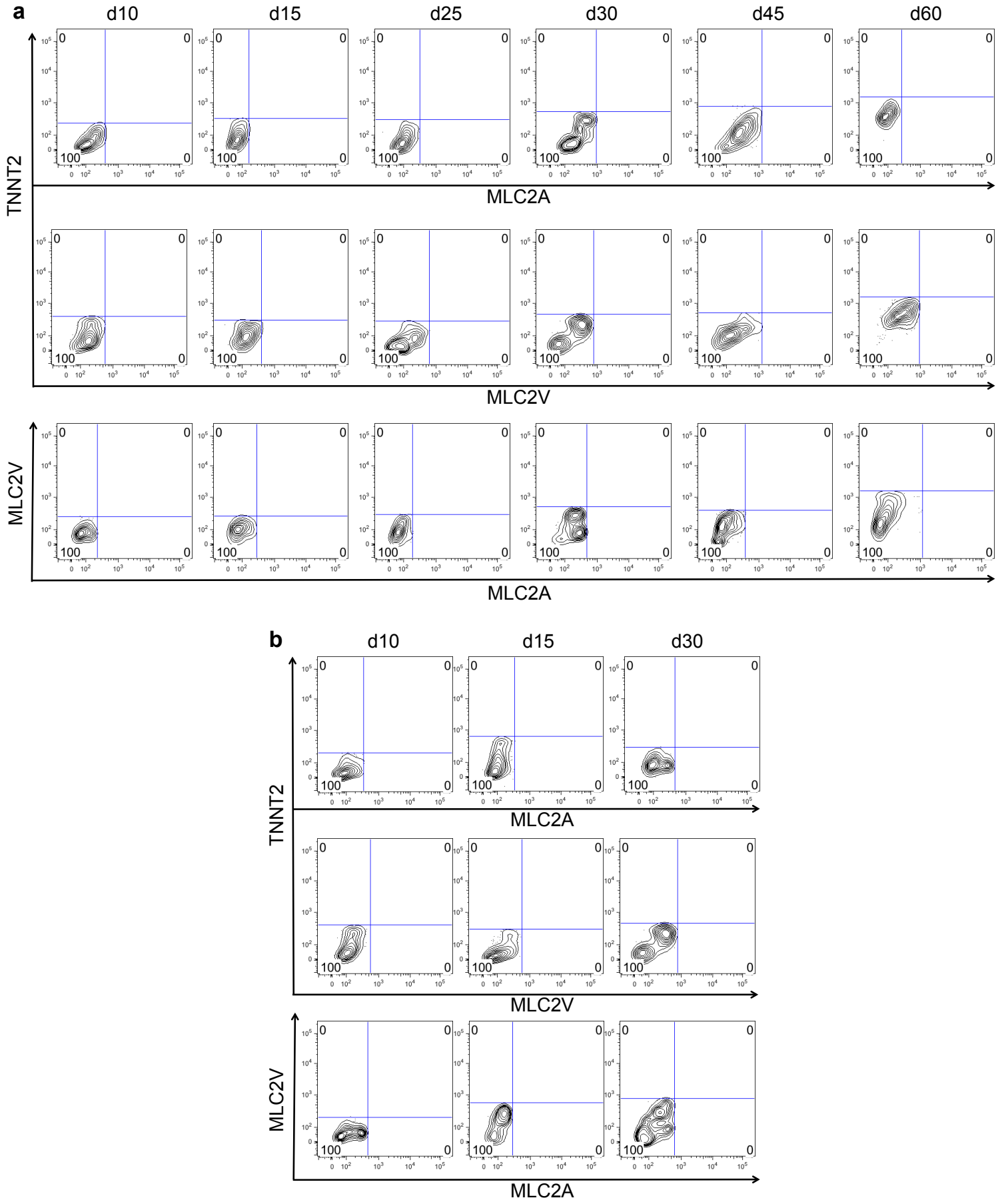

Supplementary Figure 12 | Isotype controls for TNNT2, MLC2A, and MLC2V flow cytometry assessment. **a**) Cells differentiated in CDM3. Matched to Supplementary Fig. 11a. **b)** Cells differentiated RPMI+B27-ins. Matched to Supplementary Fig. 11a.

Supplementary Table 1 | Analysis of components of defined media demonstrated effective for hESC cardiac differentiation. The constituent components of four defined media formulae, which have proven successful in either monolayer or embryoid body-based cardiac differentiation, were assessed to begin elucidation of macromolecules essential for cardiac differentiation. Concentration of L-glutamine/GlutaMAX is calculated as total in media, including any that is present in the basal media.

RPMI+B27-ins (Uosaki *et al.* 2011)[15]		LI-APEL (Elliot *et al.* 2011)[9]		StemPro-34 SFM based (Yang *et al.* 2008)[8]		Xeno-free Differentiation Medium (Burridge *et al.* 2011)[2]	
	µg/mL		µg/mL		µg/mL		µg/mL
RPMI 1640		IMDM:F12, 5% PFHMII		IMDM		RPMI	
L-glutamine (2 mM)	300	L-alanyl-L-glutamine (4 mM)	892	L-glutamine (2 mM)	300	L-glutamine (2 mM)	300
BSA	2500	Albucult	5000	HSA	5000	HSA	5000
		rH insulin	1	Human Insulin	10		
Holo transferrin	5	Holo transferrin	54	Holo transferrin	250		
Sodium selenite	0.0144	Sodium selenite	0.07	Sodium selenite	0.005		
Ethanolamine	1	Ethanolamine	203	Ethanolamine	10		
Steroids							
Corticosterone	0.02			Hydrocortisone	0.04		
Progesterone	0.0063						
Lipids							
Linoleic acid	1	Linoleic acid	0.1	Human EX-CYTE	5	Chemically defined lipids	1x
Linolenic acid	1	Linolenic acid	0.1				
Lipoic acid	0.047	Synthetic cholesterol	2.2				
Vitamins							
Retinol, all trans (vit. A)	0.1	L-ascorbic acid 2-phosphate	50	L-ascorbic acid	50	L-ascorbic acid	50
Retinol acetate (vit. A)	0.1						
D,L-a-tocopherol (vit. E)	1						
D,L-a-tocopherol acetate (vit. E)	1			D,L-a-tocopherol acetate	0.02		
Biotin (vit. B_7)	0.1						
Antioxidants							
Catalase	2.5	1-thioglycerol	49	2-mercaptoethanol	4	1-thioglycerol	49
Glutathione (reduced)	1			1-thioglycerol	49		
Superoxidase dismutase	2.5						
Other							
T3 (triiodol-l-thyronine)	0.002	Polyvinyl alcohol	500				
L-carnitine	2						
D(+)-galactose	15						
Putrescine	16.1						

Supplementary Table 2 | Optimization of minimal medium components required for efficient cardiac differentiation. **a)** Each of the 21 components of the media supplement 'B27 without insulin,' were subtracted one at a time. Results were scored 0, no cardiac differentiation or cell death; +, some contraction; ++, >50% contraction; and +++, >75% contraction. **b)** A second medium was formulated using the 10 components demonstrated to be essential in a) and each component subtracted one at a time. Only corticosterone was dispensable. **c)** Subtraction of any component from the 9-component media was not viable. **d)** Assessment of the addition of logarithmically higher or lower concentrations (x 0.1 or x 10) or the addition of components from any of the three other media formulae detailed in Supplementary Table 1. **e)** A third medium was formulated with the four increased concentrations from d) and then each component was subtracted to find which are still necessary. **f)** A fourth 6-component medium was formulated and then each component subtracted. **g)** The final 3-component medium from which CDM3 was optimized.

a		**b**		**c**		**d**		**e**		**f**		**g**	
21 components subtracting:		10 components subtracting:		9 components subtracting:		9 components with the addition of:		9 components (with 4 at 10x) subtracting:		6 components subtracting:		2 components subtracting:	
BSA	0	BSA	0	BSA	0	2 x BSA	0	BSA	0	BSA	0	BSA	0
Holo transferrin	0	Holo transferrin	0	Holo transferrin	0	10 x Holo transferrin	+	Holo transferrin	0	Holo transferrin	+++		
Sodium selenite	0	Sodium selenite	0	Sodium selenite	0	10 x Sodium selenite	+++	10 x Sodium selenite	0	10 x Sodium selenite	+++		
Ethanolamine	++												
Steroids													
Corticosterone	0	Corticosterone	++			Hydrocortisone	+						
Progesterone	++												
Lipids													
Linoleic acid	0	Linoleic acid	0	Linoleic acid	0	10 x Linoleic acid	+	Linoleic acid	0	Linoleic acid	+++		
Linolenic acid	0	Linolenic acid	0	Linolenic acid	0	10 x Linolenic acid	+	Linoleic acid	0	Linolenic acid	+++		
Lipoic acid	++					Chemically defined lipids	++						
Vitamins													
Retinol, all trans (vit. A)	++					10 x L-ascorbic acid 2-phosphate	+++	10 x L-ascorbic acid 2-phosphate	0	10 x L-ascorbic acid 2-phosphate	0	10 x L-ascorbic acid 2-phosphate	0
Retinol acetate (vit A)	0	Retinol acetate (vit A)	0	Retinol acetate (vit A)	0	10 x Retinol acetate (vit A)	+++	10 x Retinol acetate (vit A)	+++				
D,L-a-tocopherol (vit E)	++												
D,L-a-tocopherol acetate	0	D,L-a-tocopherol acetate	0	D,L-a-tocopherol acetate	0	10 x D,L-a-tocopherol acetate	+++	10 x D,L-a-tocopherol acetate	+++				
Biotin (vit B7)	++												
Antioxidants													
Catalase	++					1-thioglycerol	0						
Glutathione (reduced)	++					1-mercaptoethanol	0						
Superoxidase dismutase	++												
Other													
T3 (triiodol-l-thyronine)	0	T3 (triiodol-l-thyronine)	0	T3 (triiodol-l-thyronine)	0	10 x T3 (triiodol-l-thyronine)	+++	10 x T3 (triiodol-l-thyronine)	+++				
L-carnitine	0	L-carnitine	0	L-carnitine	0	10x L-carnitine	0						
D(+)-galactose	++					Polyvinyl alcohol	0						
Putrescine	++												

Supplementary Table 3 | Optimization of timing of Wnt signaling modulation on cardiac differentiation efficiency. **a)** Time points for the addition of GSK3B inhibitor (CHIR99021) and Wnt inhibitor (Wnt-C59) in CDM3 were modified as shown. **b)** Time points for the addition of CHIR99021 and Wnt-C59 in RPMI+B27-ins were modified as shown. Percentage of $TNNT2^+$ cells was measured at day 15 using flow cytometry; -, 0-10% $TNNT2^+$; +, 10-60% $TNNT2^+$; ++, 60-65% $TNNT2^+$; +++, 65-75% $TNNT2^+$; ++++, >75% $TNNT2^+$; Δ, media change, *n* = 2 (hiPSC line 59FSDNC3 and hESC line H7).

a

Application of small molecule inhibitors on specific days of differentiation in CDM3

d0	d1	d2	d3	d4	d5	Relative efficiency	% $TNNT2^+$
GSK3βi	WNTi			Δ		-	
GSK3βi	WNTi			Δ	Δ	-	
GSK3βi	WNTi	Δ		Δ		++	56.2±10.3
GSK3βi	WNTi	Δ		Δ	Δ	+	12.2±5.6
GSK3βi	WNTi	Δ			Δ	++	59.2±7.9
GSK3βi	Δ			WNTi		+++	68.4±15.6
GSK3βi	Δ			WNTi	Δ	+++	67.2±9.4
GSK3βi	Δ			Δ	WNTi	-	
GSK3βi	Δ	WNTi			Δ	++	60.7±7.9
GSK3βi	Δ	WNTi		Δ		++	58.4±12.4
GSK3βi	Δ	WNTi		Δ	Δ	++	60.1±15.4
GSK3βi	Δ	Δ			WNTi	-	
GSK3βi	Δ	Δ		WNTi		++	40.1±20.2
GSK3βi	Δ	Δ		WNTi	Δ	+	30.7±12.4
GSK3βi	Δ	Δ		Δ	WNTi	-	
GSK3βi		WNTi			Δ	++++	84.1±9.1
GSK3βi		WNTi		Δ		++++	86.1±10.0
GSK3βi		WNTi		Δ	Δ	++++	78.0±9.8
GSK3βi		Δ			WNTi	-	
GSK3βi		Δ		WNTi		+++	65.4±5.6
GSK3βi		Δ		WNTi	Δ	+++	61.1±13.2
GSK3βi		Δ		Δ	WNTi	-	

b

Application of small molecule inhibitors on specific days of differentiation in RPMI+B27-ins

d0	d1	d2	d3	d4	d5	Relative efficiency	% $TNNT2^+$
GSK3βi		WNTi			Δ	++	64.3±5.1
GSK3βi		WNTi		Δ		++	63.9±15.5
GSK3βi		WNTi		Δ	Δ	+	44±20.1
GSK3βi		Δ			WNTi	++++	78±4.5
GSK3βi		Δ		WNTi		++++	81.4±3.4

Supplementary Table 4 | Electrophysiological characterization of cardiomyocytes produced under chemically defined conditions. **a)** Action potential (AP) recordings using whole cell patch clamp of hiPSC-derived cardiomyocytes differentiated in CDM3 from day 15 to day 20 of differentiation. The AP characteristics used to classify cells into atrial-, nodal-, or ventricular-like. Includes MDP (maximum diastolic potential), peak voltage, APA (action potential amplitude), dV/dt_{max} (maximal rate of depolarization), and AP duration at different levels of repolarization (i.e., 90 or 50%). To determine the type of cardiomyocyte analyzed, subtypes were specified using the following characteristics: Ventricular-like, a negative maximum diastolic membrane potential (< -50 mV), a rapid AP upstroke, a long plateau phase, APA > 90 mV, and APD_{90}/APD_{50} ratio < 1.4. Atrial-like, absence of a prominent plateau phase, a negative diastolic membrane potential (< -50 mV), and APD_{90}/APD_{50} ratio > 1.7. Nodal-like, a more positive MDP, a slower AP upstroke, a prominent phase 4 depolarization, and APD_{90}/APD_{50} ratio in between 1.4-1.7. **b)** Assessment of cells differentiated in CDM3 at day 30 to 35 of differentiation. The AP characteristics used to classify cells into atrial-, nodal-, or ventricular-like (as above).

a

d15-d20

APs (*n* = 26)	Interval (s)	MDP (mV)	Peak (mV)	APA (mV)	dv/dt_{max} (V/s)	APD_{90} (ms)	APD_{50} (ms)	APD_{90}/APD_{50}
Atrial-like (*n* = 19)	0.7 ± 0.1	−55.2 ± 2.0	26.2 ± 1.2	81.3 ± 2.8	5.2 ± 0.4	140.0 ± 10.0	72.4 ± 5.0	2.0 ± 0.1
Nodal-like (*n* = 5)	0.8 ± 0.1	−45.4 ± 1.0	22.7 ± 1.5	68.1 ± 1.6	4.0 ± 0.1	135.1 ± 14.6	82.4 ± 10.0	1.7 ± 0.1
Ventricular-like (*n* = 2)	1.5 ± 0.2	−54 ± 2.0	35.9 ± 1.6	89.9 ± 3.6	7.8 ± 0.6	188.8 ± 8.3	142.3 ± 2.9	1.3 ± 0.1

b

d30-d35

APs (*n* = 13)	Interval (s)	MDP (mV)	Peak (mV)	APA (mV)	dv/dt_{max} (V/s)	APD_{90} (ms)	APD_{50} (ms)	APD_{90}/APD_{50}
Atrial-like (*n* = 4)	0.6 ± 0.2	−55.1 ± 2.4	35.7 ± 2.0	90.8 ± 3.0	6.7 ± 0.7	138.8 ± 25.0	75.3 ± 14.3	1.9 ± 0.05
Nodal-like (*n* = 2)	0.3 ± 0.01	−47.4 ± 1.0	21.7 ± 0.9	69.1 ± 1.3	2.9 ± 0.1	73.9 ± 1.1	48.9 ± 0.10	1.5 ± 0.02
Ventricular-like (*n* = 7)	0.4 ± 0.04	−57.8 ± 1.7	41.0 ± 3.4	98.8 ± 3.3	9.2 ± 0.6	218.7 ± 46.2	192.5 ± 44.3	1.2 ± 0.03

Supplementary Table 5 | Taqman gene expression assays used for time course real time RT-PCR

Category	Gene symbol	TaqMan assay
Housekeeping	*18S*	Hs99999901_s1
Pluripotency	*NANOG*	Hs02387400_g1
	POU5F1	Hs00999632_g1
	SOX2	Hs01053049_s1
	KLF4	Hs00358836_m1
	LIN28	Hs00702808_s1
	MYC	Hs00153408_m1
	UTF1	Hs00747497_g1
	ABCG2	Hs01053790_m1
	DMNT3B	Hs01002405_m1
Mesoderm	*TERT*	Hs99999022_m1
	TP53	Hs99999147_m1
Cardiac mesoderm	*MESP1*	Hs00251489_m1
Cardiac development	*KDR*	Hs00176676_m1
	MEF2C	Hs00231149_m1
	GATA4	Hs00171403_m1
	ISL1	Hs01099687_m1
	TBX5	Hs00361155_m1
	NKX2-5	Hs00231763_m1
Cardiac structure	*TNNT2*	Hs00165960_m1
	MYH6	Hs00411908_m1

Supplementary Table 6 | Taqman gene expression assays used for single cell real time RT-PCR

Category	Gene symbol	TaqMan assay
Housekeeping	*18S*	Hs99999901_s1
	GAPDH	Hs99999905_m1
Pluripotency	*ZFP42*	Hs00399279_m1
Ectoderm	*SOX3*	Hs00271627_m1
Endoderm	*FOXA2*	Hs00232764_m1
Mesoderm	*T (Brachyury)*	Hs00610080_m1
	MIXL1	Hs00430824_g1
Cardiac development	*NKX2-5*	Hs00231763_m1
	ISL1	Hs01099687_m1
Cardiac structure	*TNNT2*	Hs00165960_m1
	MYH6	Hs00411908_m1
	MYH7	Hs01110632_m1
	TNNI3	Hs00165957_m1
Atrial/ventricular	*MYL7 (MLC2a)* - constitutive	Hs01085598_g1
	MYL2 (MLC2v) - ventricular	Hs00166405_m1
	NPPA (ANP) - atrial	Hs00383230_g1
	NPPB (BNP) – constitutive	Hs01057466_g1
	SLN - atrial	Hs01888464_s1
	IRX4 - atrial	Hs00212560_m1
Nodal	*TBX18* - nodal	Hs01385457_m1
Gap junction	*Connexin-40 (GJA5)* - atrial	Hs00270952_m1
	Connexin-43 (GJA1) - ventricular	Hs00748445_s1
Ion channels	*HCN1*	Hs01085412_m1
	HCN4	Hs00175760_m1
	KCNQ1	Hs00923522_m1
	KCNH2	Hs04234270_g1
	KCNJ2	Hs00265315_m1
	RYR2	Hs00892842_m1
	SCN5A	Hs00165693_m1
	CACNA1C	Hs00167681_m1
	CACNA1H	Hs00234934_m1
Adrenoreceptors	*ADRA1A*	Hs00169124_m1
	ADRA1B	Hs00171263_m1
	ADRA1D	Hs00169865_m1
	ADRB1	Hs00265096_m1
	ADRB2	Hs00240532_s1